Investigation of Corrosion Inhibition Activity of 3-butyl-2,4,5-triphenylimidazole and 3-butyl-2-(2-butoxyphenyl)-4,5-diphenylimidazole toward Carbon Steel in 1% NaCl Solution

Megawati Zunita[*] *, Deana Wahyuningrum, Buchari, Bunbun Bundjali*

Department of Chemistry, Faculty of Mathematics and Natural Sciences, Institut Teknologi Bandung
Jalan Ganesha 10, Bandung 40132, Jawa Barat, Indonesia
[*]E-mail: megazunita.105@gmail.com

Overcoming of corrosion problem on the surface of carbon steel is still being developed until present. The recent publications showed that the corrosion inhibitor with good hydrophobic properties and strong interaction with the carbon steel surface is needed. Therefore, 3-butyl-2,4,5-triphenylimidazole and 3-butyl-2-(2-butoxyphenyl)-4,5-diphenylimidazole were synthesized to be applied as corrosion inhibitors. The synthesis of 3-butyl-2,4,5-triphenylimidazole (**1**) and 3-butyl-2-(2-butoxyphenyl)-4,5-diphenylimidazole (**2**) were carried out by a Microwave Assisted Organic Synthesis (MAOS) method. The results of Electrochemical Impedance Spectroscopy (EIS) measurements show that the adsorption mechanism of 3–butyl–2,4,5-triphenylimidazole and 3–butyl–2-(2-butoxyphenyl)-4,5-diphenylimidazole onto carbon steel surface obeyed Langmuir adsorption isotherm with the value of ΔG_{ads} are -34.49 kJ.mol^{-1} and -40.19 kJ.mol^{-1}, respectively, which correspond to the spontaneous interaction between corrosion inhibitors and carbon steel surface by semi-chemisorptions and chemisorptions interaction.

1. INTRODUCTION

Corrosion can be interpreted as a destructive attack of metal because of the chemically or electrochemically reaction of metal and the environment [1]. Corrosion in the aquatic environment and in the open air (which is surrounded by a layer of water) is an electrochemical process, because the corrosion involves electron transfer between the metal surface and electrolyte solution [2].

The corrosion that occurs in the inner surface of carbon steel pipelines used in oil and gas industries is the primary cause of leakage and it will cause danger to every living thing. Furthermore, corrosion causes various inconvenient effects to the national income [3]. The loss caused by corrosion has forced experts in the corrosion field worldwide to develop methods to handle it. Cathodic and anodic protection, coating of metal surface by painting or plating, and the manufacturing of corrosion inhibitors are the several methods that have been done by the experts to solve the problems [4]. Anodic/cathodic protection and coating of metal surfaces can be done in order to protect the outer surface of carbon steel pipelines. However, the prevention of corrosion which occurs in the internal parts of carbon steel pipelines cannot be done effectively by either anodic and cathodic protection or coating method. Therefore, corrosion inhibitors have been developed in order to protect the inner surface of the pipelines, especially the carbon steel pipelines in oil and gas industry.

Currently, developments of corrosion inhibitors have led to the utilizing of organic compounds because they are more environmentally friendly, relatively cheap, and more effective in their corrosion inhibition ability than the inorganic ones. One of the requirements in which an organic compound must have to be used as a corrosion inhibitor is the presence of lone pair electrons that facilitates the interaction between the compound and carbon steel surface [3]. The acidic corrosion inhibitors which often used in industry are organic compounds with double bonds and the lone pairs electrons that can make interaction with a metal surface, such as the lone pairs electrons of nitrogen, sulfur, and oxygen atom [5,6]. Corrosion inhibition depends on the strength of active adsorption centers. Inhibition efficiency of hetero-compounds follow the order $O < N < S < P$ [4].

Imidazole is an organic compound which has a heterocyclic structure with molecular formula of $C_3H_4N_2$. Imidazole compound and its derivatives contain N functional groups with lone pairs electrons and the resonance system within the aromatic ring that facilitates their interaction with carbon steel surface. Many imidazole derivative compounds have been synthesized because of their low toxicity and environmentally friendly properties [7]. Therefore, two imidazole derivative compounds, which are 3-butyl-2,4,5-triphenylimidazole (**1**) and 3-butyl-2-(2-butoxyphenyl)-4,5-diphenylimidazole (**2**), have been synthesized in this research to be applied as corrosion inhibitors.

The synthesis of compound **1** and **2** utilized Microwave Assisted Organic Synthesis (MAOS) method, a relatively 'green', effective, and efficient method to synthesis various compounds, either inorganic or organic ones [8]. This method utilizes the microwave to carry out chemical reactions based on the polarity of compounds, especially when the compounds are interacting with the microwave energy [8].

2. EXPERIMENTAL PART

2.1. Materials

The materials used for synthesis were obtained from Merck and directly used without any further purification.

Materials used for synthesis were benzaldehyde, salicylaldehyde, thiamine chloride, ethanol, acetic acid glacial, acetone, copper acetate, ammonium hydroxide, ammonium acetate, acetonitrile, DMF (*N,N*-dimethylformamide), bromobutane, KOH, NaOH, filter paper, NaCl, aqua demineralization, n-hexane, ethyl acetate, aluminum TLC plates of silica gel GF_{254}, Celite, carbon steel coupons with the following composition (in percent,%): Fe (99.5756), Mn (0.22984), C (0.05991), Al (0.04752), Si (0.02986), Cr (0.01895), P (0.0123), S (0.00731), Cu (0.0066), Ni (0.0046), Mo (0.003), V (0.00291), Ti (0.00252), Zn (0.00237), Pb (0.0022), Sn (0.00136), Nb (0.00117), W (0.00009) [7], and carbondioxide gas.
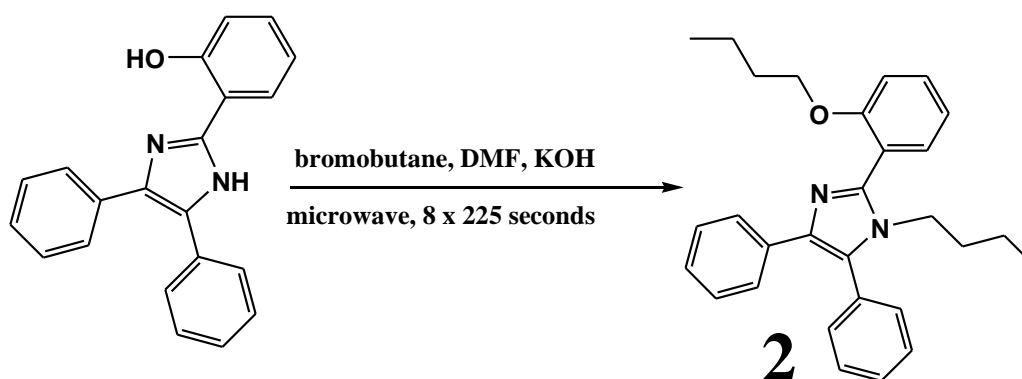
2.2. Experimental Procedure

2.2.1 Synthesis of Compound *1* and *2*

The synthesis of compound **1** and **2** was carried out using MAOS (Microwave Assisted Organic Synthesis) method modified from previous research as shown in scheme 1 and 2 [9,10].
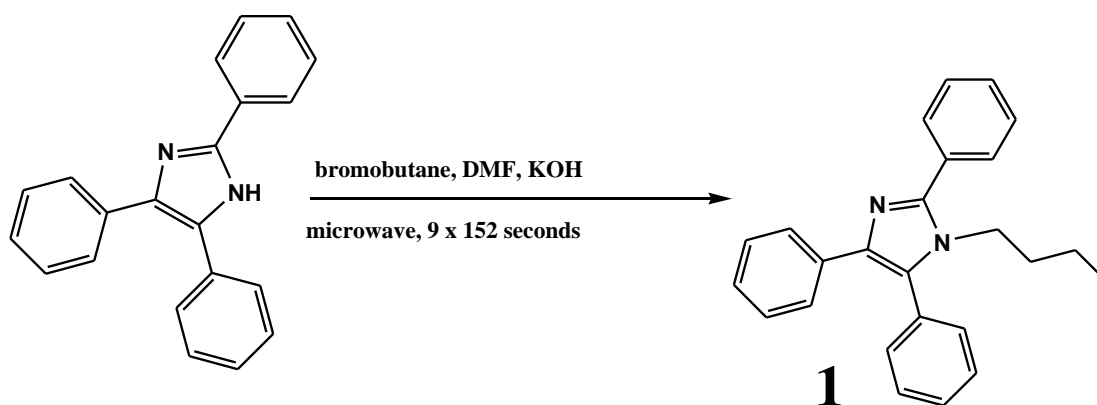
Scheme 1.

Scheme 2.

Precursor compound (2 mmol), which are 2,4,5-triphenylimidazole and 2-(2-hydroxyphenyl)-4,5-diphenylimidazole for synthesizing compound **1** and **2** respectively, was mixed with potassium hydroxide (KOH) (4 mmol), then bromobutane (2 mmol and 4 mmol for synthesizing compound **1** and **2**, respectively) and DMF (100 mL) were added. The mixtures were reacted in a microwave oven (Sharp R-248J(S) microwave oven) and the temperature was controlled until the reaction is complete using infrared thermometer (Lutron TM-919A infrared thermometer). During the reaction, once every 152 seconds and 225 seconds, respectively for compound **1** and **2,** the reaction process was checked by thin layer chromatography (TLC) using n-hexane:ethyl acetate 7:3 as eluents. After the reactions have been completed, the mixtures were cooled to room temperature. The synthesized product was a mixture of liquid and solid materials so that they were separated by decantation process. The liquid phase was purified utilized preparative thin layer chromatography while the solid phase was dissolved in ethyl acetate and further purified by preparative thin layer chromatography. The thin layer chromatography was then extracted. The purification has done by the vacuum filtration method using Celite, after previously drying it out through anhydrous Na_2CO_3, and then the filtrate was concentrated. The results from the preparative thin layer chromatography separation process, both the filtrate and solid products, were characterized using IR, MS, and NMR.

The crystal of compound **1** is yellowish with chemical yields of 32.18%. IR spectra measured by JASCO FT/IR-5000 spectrophotometer and Buck Scientific Model 500 IR spectrophotometer (KBr) showed peaks at wavenumbers of 1462.04, 1487.12, 1597.06, and 3488.72 cm^{-1}; ^{1}H NMR spectrum (JEOL NMR JNM ECA- 500 spectrometer) (500 MHz, DMSO-d_6) showed chemical shifts (δ, ppm) at 0.93 (*m*, 3H), 1.29 (m, 2H), 1.61 (*dd*, 2H), 3.23 (*dd*, 2H), 7.35 (*d*), 7.53(*d*), and 7.79(*d*) (characteristics of the signal peaks from protons located at three benzene ring is almost symmetric in compound **1**); ^{13}C NMR spectrum (125 MHz, DMSO-d_6) showed chemicals shifts (δ, ppm) at 19.2, 30.1, 33.0, 128.6, 129.6, 127.4, 131.2, 129.1, 130.7, and 142.6; ESI-MS (LCT Premier XE ESI-MS) [M+H]$^+$ m/z: 353.2017 ($C_{25}H_{25}N_2$).

The crystal of compound **2** is yellowish brown with chemical yields of 28.12%; IR bands (JASCO FT/IR-5000 spectrophotometer and Buck Scientific Model 500 IR spectrophotometer)(KBr): 1255.69, 1498.69, 1668.43, and 2929.87 cm^{-1}; ^{1}H NMR spectrum (JEOL NMR JNM ECA- 500 spectrometer) (500 MHz, DMSO-d_6): δ ppm 0.92 (*m*, 3H), 1.37 (*dd*, 2H), 1.65 (*dd*, 2H), 3.64 (*dd*, 2H), 1.64 (*dd*, 2H), 4.04(*dd*, 2H), 7.09, 7.05, 7.06, 7.18, 7.56, 7.38, and 7.30 (characteristics of the signal peaks from protons located at three benzene ring is also almost symmetric in compound **2**); ^{13}C NMR spectrum (125 MHz, DMSO-d_6): δ ppm 12.9, 23,7, 31.6, 44.0, 13.6, 18,7, 30.7, 67.6, 112.5, 129.2, 120.6, 125.8, 128.1, 156.5, 144.7, 131.9, 134.9, 136.2, 125.9, 128.8, and 128.0; ESI-MS (LCT Premier XE ESI-MS) [M+H]$^+$ m/z: 425.1172 ($C_{29}H_{32}N_2O$).

2.2.2 Electrochemical measurements by EIS method

Blank was prepared by providing an electrolyte solution of 1% (w/v) NaCl in accordance with the solvent used to dissolve the compounds synthesized. A total of 100 mL 1% (w/v) NaCl electrolyte solution (blank) were placed in 250 mL beaker equipped with a magnetic stirrer bar and electrodes.

The electrodes used are carbon steel electrode as working electrode, platinum electrode as auxiliary electrode and saturated calomel electrode as reference electrode. The CO_2 gas was bubbling into the solution for 30 minutes to ensure that CO_2 has been saturated in the solution and then the measurements began. After blank solution were measured over the Nyquist mode of EIS measurements, then it was injected with different concentrations of inhibitor, starting from the lowest to the highest concentration without changing blank solution. The Nyquist curve was performed for every addition of corrosion inhibitor into the blank solution.

3. RESULTS AND DISCUSSION

Both imidazole derivative compounds, 3-butyl-2,4,5-triphenylimidazole (**1**) and 3-butyl-2-(2-butoxyphenyl)-4,5-diphenylimidazole (**2**), have been successfully synthesized utilizing MAOS method, which was a modification of the method presented by Handy and Okello [9]. The structures of products were presented on Figure 1.
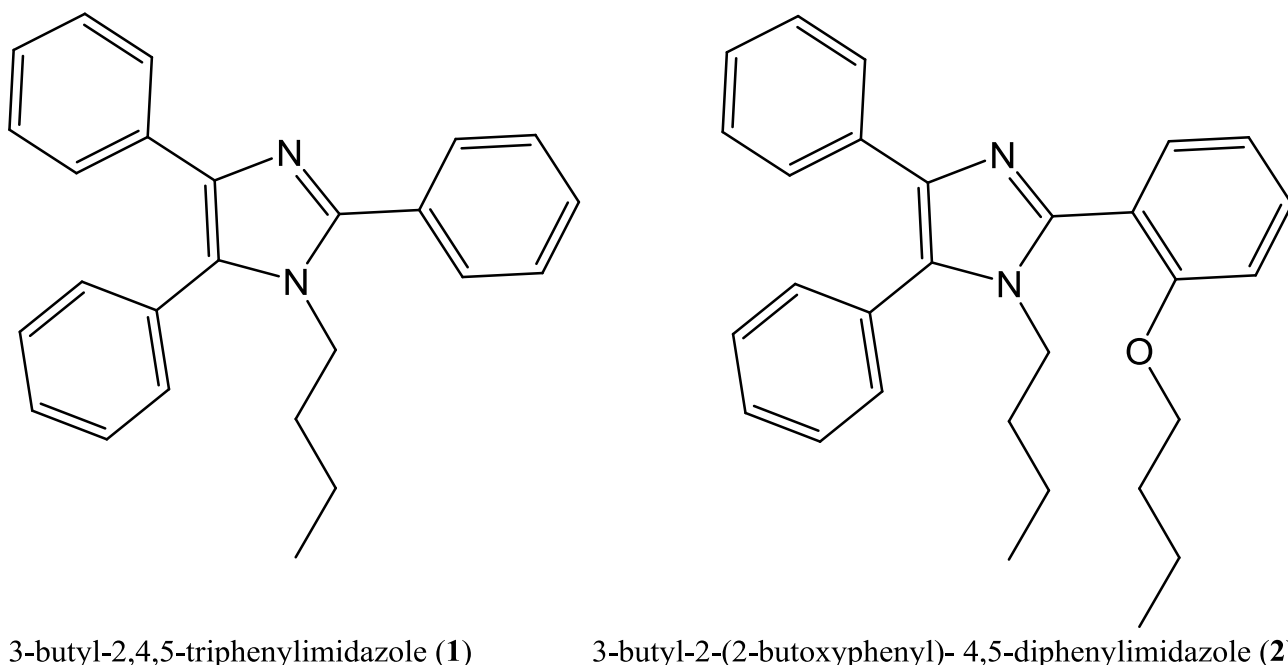

3-butyl-2,4,5-triphenylimidazole (**1**)   3-butyl-2-(2-butoxyphenyl)- 4,5-diphenylimidazole (**2**)

Figure 1. The structures of novel synthesized corrosion inhibitors

Investigation of compound **1** and **2** as corrosion inhibitors were carried out using EIS method at various concentrations in 1%(w/v) NaCl solution and various temperatures. Both of these compounds were tested for their ability as corrosion inhibitor towards carbon steel in 1%(w/v) NaCl solution, in order to reveal the influence of the butyl side chains within both compounds towards their ability to inhibit the corrosion process. The corrosion inhibition activity measurement results using EIS method produced the data of resistance of the system solution, R_p, in ohm, at various concentrations of corrosion inhibitor and various temperatures, which was presented in Table 1 and 2.

Table 1. The data of resistance of the system solution, R_p, in ohm, at various concentrations of compound **1** and various temperatures obtained from the EIS measurements

Temperature (^{o}C)	R_p (ohm)					
	Blank	8 ppm	10 ppm	20 ppm	40 ppm	60 ppm
25	219.6	269.3	299.1	305.6	315.7	330.0
35	122.2	134.0	219.2	282.7	226.3	149.8
45	107.4	120.2	175.4	189.36	199.7	177.3
55	69.78	78.19	90.36	76.80	77.43	72.31

Table 2. The data of resistance of the system solution, R_p, in ohm, at various concentrations of compound **2** and various temperatures obtained from the EIS measurements

Temperature (^{o}C)	R_p (ohm)					
	Blank	8 ppm	10 ppm	20 ppm	40 ppm	60 ppm
25	155.4	271.6	286.9	397.1	358.5	336.6
35	121.9	218.4	250.7	265.3	260.4	256.0
45	66.16	76.43	85.40	89.36	99.70	77.30
55	61.78	76.19	80.36	74.80	67.43	64.68

The data of corrosion inhibition efficiency test by EIS method of imidazole derivatives compounds was shown in the Table 3 and Table 4. The percentages of corrosion inhibition efficiency (%IE) can be obtained using the following equation [11,12].

$$\% \text{ IE (Inhibition efficiency)} = 1 - \frac{R_{p(u)}}{R_{p(i)}} \times 100\% \tag{1}$$

where $R_{p(u)}$ and $R_{p(i)}$ are the representatives of the resistance of uninhibited and inhibited system, respectively.

Table 3. Corrosion inhibition efficiency of compound **1** towards carbon steel in 1% (w/v) NaCl solution at various concentrations and temperatures

Temperature (^{o}C)	%IE				
	8 ppm	10 ppm	20 ppm	40 ppm	60 ppm
25	18.46	26.58	28.14	30.44	33.45
35	8.81	44.25	56.77	46.00	18.42
45	10.65	38.77	43.28	46.22	39.42
55	10.76	22.78	9.14	9.88	3.50

Table 4. Corrosion inhibition efficiency of compound **2** towards carbon steel in 1 %(w/v) NaCl solution at various concentrations and temperatures

Temperature (°C)	% IE				
	8 ppm	10 ppm	20 ppm	40 ppm	60 ppm
25	42.78	45.83	60.87	56.65	53.83
35	44.18	51.38	54.05	53.19	52.38
45	13.44	22.53	25.96	33.64	14.41
55	18.91	23.12	17.41	8.38	4.48

The obtained data from the EIS measurements of the corrosion inhibition efficiency showed that the corrosion inhibition efficiencies of both compounds were increased after the addition of inhibitor into blank solution. These results suggest that the resistance of inhibited solution towards corrosion process on the surface of carbon steel increased as a result of the formation of inhibitor layer on carbon steel surface, whereas in the uninhibited condition the resistance of solution towards corrosion process decreased. Figure 2 and 3 are the representation of Nyquist curves derived from the EIS measurements, which showed that the impedance of carbon steel surfaces against corrosion increased after the addition of corrosion inhibitor. Compound **1** is more effective corrosion inhibitor when used at temperatures of 35°C, whereas compound **2** is more effective to be used as corrosion inhibitor at 25°C. These facts were confirmed by the large value of % IE of each compound as presented in Table 3 and 4. The increase of temperature generally caused the decrease in corrosion inhibition efficiency of both compounds at various concentrations which led to the assumption that mainly the interaction between inhibitors and carbon steel surface would be physical attraction.
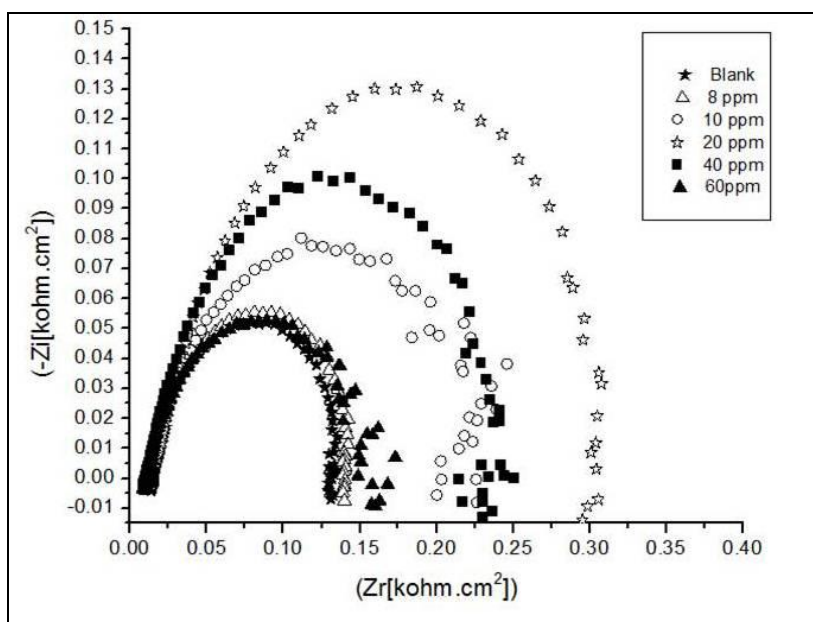

Figure 2. The Nyquist curves obtained from the corrosion inhibition activity measurements of compound **1** using EIS method at temperature of 35°C
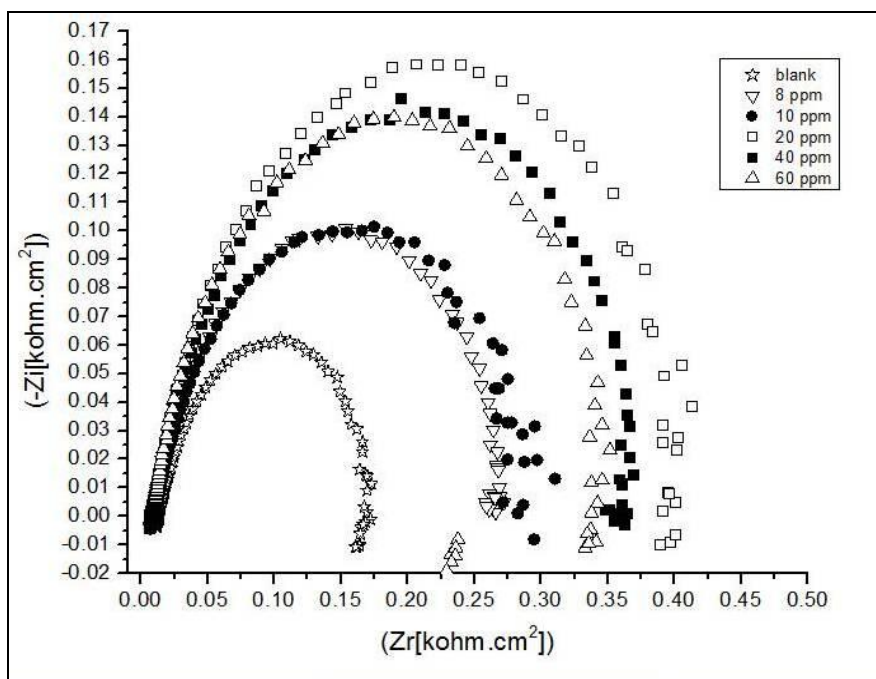
Figure 3. The Nyquist curves obtained from the corrosion inhibition activity measurements of compound **2** using EIS method at temperature of 25 ^{o}C

The results presented on Table 3 and 4 showed that 3-butyl-2,4,5-triphenylimidazole (**1**) and 3-butyl-2-(2-butoxyphenyl)-4,5-diphenylimidazole (**2**) have the potent as corrosion inhibitor. The best of corrosion inhibition efficiency so far for compound **1** and **2** at the same concentration (20 ppm) were 56.77% at 35 °C and 60.87% at 25 °C, respectively.

The adsorption mechanism of compound **1** and **2** on carbon steel surface was also determined. The adsorption mechanism generally occurred on the surface of carbon steel are corresponded to the Langmuir and Temkin adsorption isotherms, because corrosion inhibitors can interact with the surface of carbon steel as the form of gas phase. Initially corrosion inhibitors were made to become gas phase in order to form a thin layer on the surface of carbon steel. In this study, the most appropriate relationship between the concentrations of corrosion inhibitor compounds, C_{inh}, and the degree of surface coverage, θ, is the simple form of Langmuir adsorption isotherm, according to the following equation [11,12].

$$\theta = \frac{bC_{inh}}{1+bC_{inh}} \qquad (2)$$

where θ is the degree of surface coverage, b is the adsorption coefficient, and C_{inh} is the concentration of inhibitor.

The calculation results based on the EIS measurements data of compound **1** and **2** as listed on Table 5 and 6 using eq. 2 yields θ, C/θ, and ln C to be plotted as shown on Figure 4 and Figure 5.
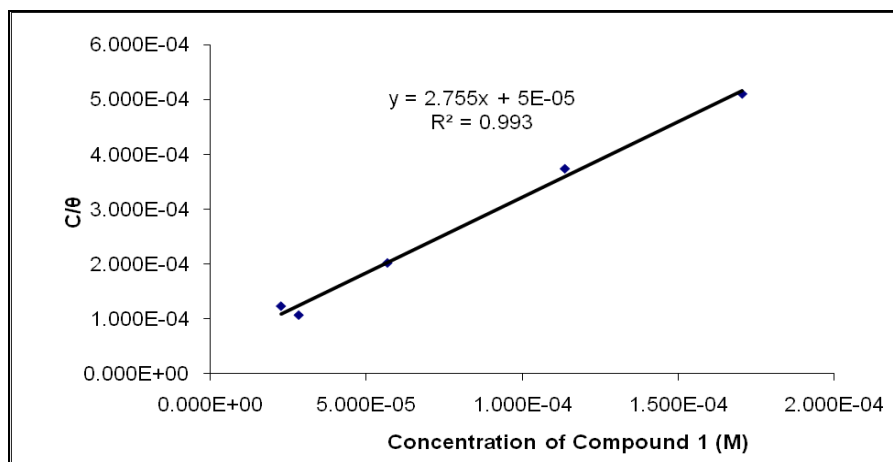
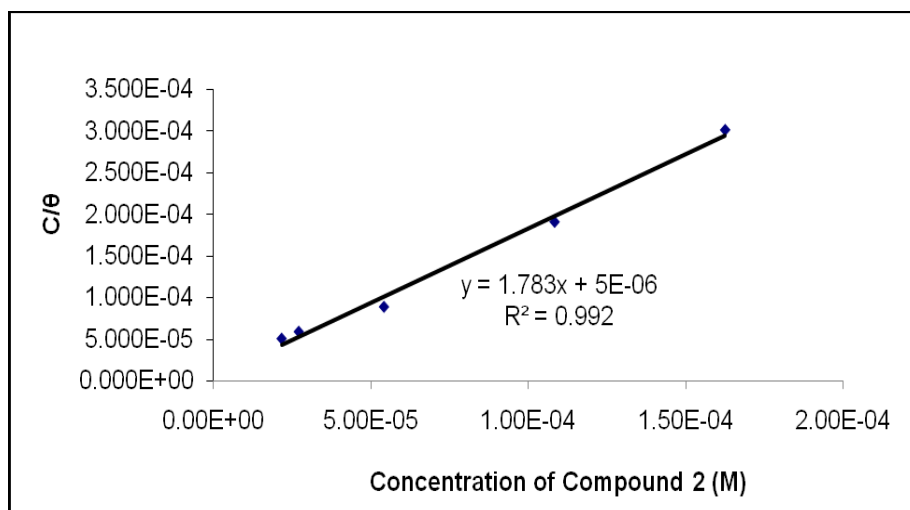**Figure 4.** The plot of Langmuir adsorption isotherm of compound **1** at 25°C

Figure 5. The plot of Langmuir adsorption isotherm of compound **2** at 25°C

Table 5. Data of θ, C/θ, and ln$C$ obtained from the measurement of inhibition capability of compound **1** using EIS method at 25°C

C,Concentration of Compound **1** (ppm)	C,Concentration of Compound **1** (M)	R_2	%IE	θ	C/θ	ln$C$
Blank		219.6				
8 ppm	2.273E-05	269.3	18.46	0.18455	1.231E-04	-10.6919
10 ppm	2.841E-05	299.1	26.58	0.26580	1.069E-04	-10.4688
20 ppm	5.682E-05	305.6	28.14	0.28141	2.019E-04	-9.77565
40 ppm	1.136E-04	315.7	30.44	0.30440	3.733E-04	-9.08251
60 ppm	1.705E-04	330.0	33.45	0.33455	5.095E-04	-8.67704

Table 6. Data of θ, C/θ, and $\ln C$ obtained from the measurement of inhibition capability of compound **2** using EIS method at 25°C

C,Concentration of Compound **2** (ppm)	C,Concentration of Compound **2** (M)	R_2	% IE	θ	C/θ	$\ln C$
Blank		155.4				
8 ppm	2.168E-05	271.6	42.78	0.42784	5.067E-05	-10.7391
10 ppm	2.710E-05	286.9	45.83	0.45835	5.913E-05	-10.5159
20 ppm	5.420E-05	397.1	60.87	0.60866	8.905E-05	-9.8228
40 ppm	1.084E-04	358.5	56.65	0.56653	1.913E-04	-9.1297
60 ppm	1.626E-04	336.6	53.83	0.53832	3.021E-04	-8.7242

The value of free Gibbs adsorption energy (ΔG_{ads}, in kJ/mol) of each compound, can be determined using the following equation [11,12]

$$K_{ads} = \frac{\theta}{C(1-\theta)} \tag{3}$$

$$\Delta G_{ads} = -RT \ln(55.55 K_{ads}) \tag{4}$$

Table 7. The value of free Gibbs adsorption energy (ΔG_{ads}, in kJ/mol) obtained from data calculation based on theoretical determination of the Langmuir adsorption isotherms plot (Fig.4) of compound **1**

Slope value	Intercept value	$K_{ads} = (1/\text{intercept value})(M^{-1})$	ΔG_{ads} (kJ/mol)
2.7559	5.00×10^{-5}	2.00×10^{4}	-34.49

Table 8. The value of free Gibbs adsorption energy (ΔG_{ads}, in kJ/mol) obtained from data calculation based on theoretical determination of the Langmuir adsorption isotherms plot (Fig.5) of compound **2**

Slope value	Intercept value	$K_{ads} = (1/\text{intercept value})(M^{-1})$	ΔG_{ads} (kJ/mol)
1.783	5.00×10^{-6}	2.00×10^{5}	-40.19

The obtained data showed that the adsorption mechanism of compound **1** and **2** on carbon steel surface follows Langmuir adsorption isotherm mechanism with data consistency value approaching to 1, which were 0.993 and 0.992, respectively. The value of ΔG_{ads} of compound **1** is -34.49 kJ/mol, and it corresponds to semi-chemisorption/semi-physiosorption mechanism, whereas ΔG_{ads} of compound **2** is -40.19 kJ/mol which indicates that the adsorption of compound **2** on the surface of carbon steel occurs in chemisorptions (chemical adsorption) mechanism. If the value of ΔG_{ads} is more positive than

-20 kJ/mol, then it would facilitate physiosorption interaction between corrosion inhibitor and carbon steel surface. Otherwise, if ΔG_{ads} is more negative than -40kJ/mol, then it may leads to the chemisorptions interaction between inhibitor corrosion and carbon steel surface [13].
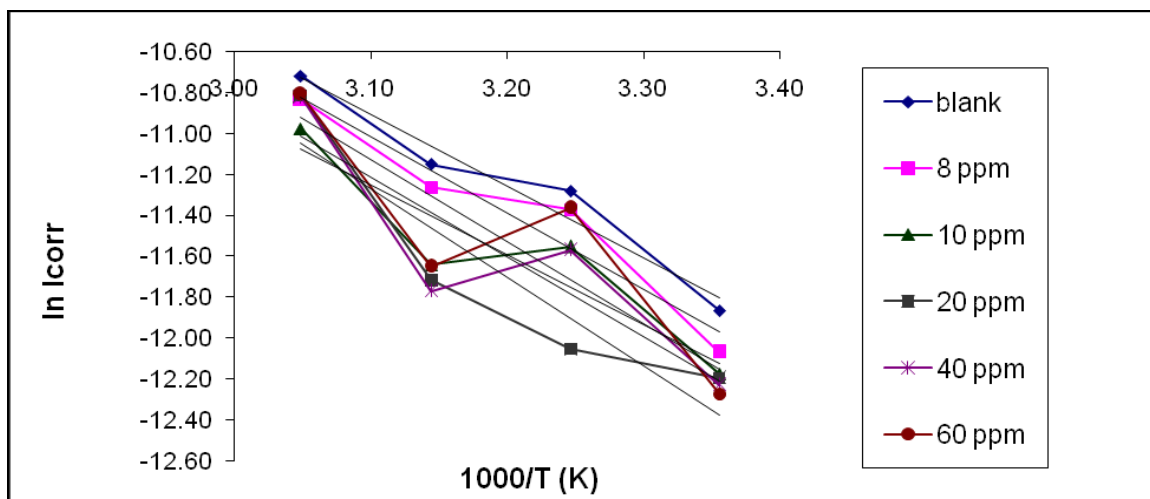

Figure 6. The relationship between $\ln(I_{corr})$ of compound **1** and 1000/T to determine the activation energy of corrosion process in the uninhibited and inhibited system (on the addition of compound **1** at various concentrations) .
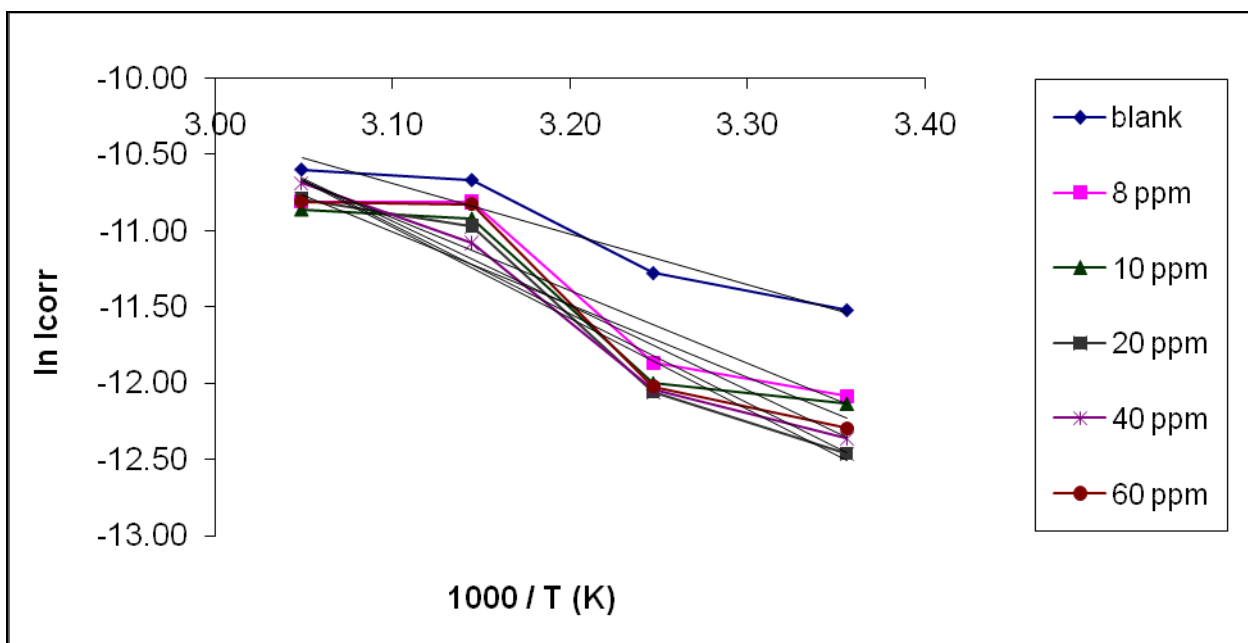

Figure 7. The relationship between $\ln(I_{corr})$ of compound **2** and 1000/T to determine the activation energy of corrosion process in the uninhibited and inhibited system (on the addition of compound **2** at various concentrations)

The determination of the kinetics of the corrosion rate due to the presence and the absence of corrosion inhibitor in terms of activation energy value utilized the following equation [11,12].

$$\ln(I_{corr}) = \ln A - \frac{E_a}{RT} \tag{5}$$

Where I_{corr} is the current density of corrosion rate of the system; A is the Arrhenius constant which is determined empirically, E_a is the activation energy of corrosion process (kJ/mol), R is the ideal gas constant (8.314 J.mol^{-1}K^{-1}), and T is temperature (K). The linear representation of eq. 5 is expressed as follows:

$$\ln(I_{corr}) = \left[-\frac{E_a}{R}\right]\frac{1}{T} + \ln A \tag{6}$$

The data on Table 5 and 6 was recalculated and plotted as shown on Figure 6 and 7.

The activation energy data after the addition of compound **1** and **2** to 1%(w/v) NaCl solution at various concentrations are summarized in the following Table 9 and Table 10.

Table 9. The activation energy data of corrosion system before and after the addition of compound **1**

E_a (kJ/mol)	Blank	8 ppm	10 ppm	20 ppm	40 ppm	60 ppm
	29.07	31.16	28.44	36.00	32.47	33.39

Table 10. The activation energy data of corrosion system before and after the addition of compound **2**

E_a (kJ/mol)	Blank	8 ppm	10 ppm	20 ppm	40 ppm	60 ppm
	27.52	39.61	39.77	49.62	48.46	46.01

The activation energy data shown in Table 9 and 10 indicates that the rate of corrosion in the system decreased after corrosion inhibitor added. Before the addition of compound **1** and **2**, the activation energies of each uninhibited system are 29.07 kJ.mol^{-1} and 27.52 kJ.mol^{-1}, respectively. After the addition of corrosion inhibitor, the activation energy of corrosion system increased. These results show that the energy required to achieve equilibrium of corrosion process in the inhibited systems is higher than in uninhibited system, therefore the corrosion inhibitors has successfully inhibited the rate of corrosion in the system. The most efficient concentration used to inhibit the rate of corrosion is 20 ppm with the activation energy values, E_a, of compound **1** and **2** are 36.00 kJ.mol^{-1} and 49.62 kJ.mol^{-1}, respectively.

Thermodynamic parameter of corrosion processes is essential to know the spontaneity of corrosion reaction in the system. The values of thermodynamic parameters from EIS data can be used to determine the performance of corrosion inhibitors in inhibiting the corrosion rate. Thermodynamic parameters can be obtained from the following equation [11,12].

$$\ln \frac{I_{corr}}{T} = \ln \frac{R}{Nh} + \frac{\Delta S^*}{R} - \frac{\Delta H^*}{RT} \tag{7}$$

$$I_{corr} = \frac{K}{R_p L} \tag{8}$$

where K is a constant value determined empirically which is 0.02 V, R_p is the resistance in the system (ohm.cm^2) and L is the diameter of the metal used during the test (mm). The representative graphic describing the linear relationship between $\ln(I_{corr}/T)$ and $1 / T$ utilized the following linear equation.

$$\ln \frac{I_{corr}}{T} = \left[-\frac{\Delta H^*}{R} \right] \frac{1}{T} + \left[\ln \frac{R}{Nh} + \frac{\Delta S^*}{R} \right] \tag{9}$$

The thermodynamic parameters shown in Table 11 and Table 12 indicate the spontaneity of the formation of the corrosion activated state that leads to the spontaneity of corrosion process in the uninhibited system, which is indicated by the values of ΔH*, ΔS* which are lower than the inhibited system, and the values of ΔG* are higher than in the inhibited system.

Table 11. Data of thermodynamic parameters of corrosion process in the uninhibited and inhibited system (on the addition of compound **1**)

Solution	ΔH* (kJ/mol)	ΔS* (J/mol)	ΔG* (kJ/mol)			
			25°C	35°C	45°C	55°C
Blank	29.07	-245.49	73.19	75.64	78.09	80.55
8 ppm	31.16	-239.88	71.52	73.92	76.31	78.71
10 ppm	28.44	-250.25	74.60	77.11	79.61	82.11
20 ppm	35.99	-227.00	67.68	69.95	72.22	74.49
40 ppm	32.47	-237.45	70.79	73.17	75.54	77.92
60 ppm	33.39	-233.91	69.74	72.08	74.42	76.75

The role of corrosion inhibitor in the prevention of corrosion reactions in the system can be seen from the data of thermodynamic parameters in Table 11 and Table 12. The ΔH* values of the inhibited systems, which each of it contains compound **1** and **2** as inhibitor, are higher than in the uninhibited system, which indicates that the corrosion process requires higher energy to reach the equilibrium or activated state. The ΔS* values of the inhibited systems, are also higher than in the

uninhibited system, which indicates that the degree of disorder in the system increases and lead to the inhibition of the rate of corrosion. The ΔG^* values of the inhibited systems are lower than the in the uninhibited system, which indicates that the corrosion inhibition reaction proceeds spontaneously after the addition of a corrosion inhibitor. The comparison of the thermodynamic parameters of both compounds shows that the activity of compound **2** as corrosion inhibitor is better than compound **1**.

Table 12. Data of thermodynamic parameters of corrosion process in the uninhibited and inhibited system (on the addition of compound **2**)

Solution	ΔH^* (kJ/mol)	ΔS^* (J/mol)	ΔG^* (kJ/mol)			
			25°C	35°C	45°C	55°C
Blank	27.52	-248.44	74.06	76.55	79.03	81.52
8 ppm	39.61	-212.88	63.48	65.61	67.74	69.86
10 ppm	39.77	-213.07	63.53	65.67	67.80	69.93
20 ppm	49.62	-182.34	54.39	56.21	58.03	59.86
40 ppm	48.46	-185.81	55.42	57.28	59.14	60.99
60 ppm	46.01	-193.21	57.62	59.55	61.49	63.42

Based on all of the analysis, the interactions between compound **1** and carbon steel surface are formed from the lone pair electrons from nitrogen atoms and the delocalized electrons of aromatic ring to facilitate the interaction of the compound with carbon steel. Therefore, the carbon steel was covered by the layers of compound **1** and the oxidation rate on the surface of carbon steel was decreased. Whereas the adsorption of compound **2** on carbon steel surface, in addition to the interaction between the lone pair electrons from nitrogen atoms as well as the delocalized electrons of aromatic ring with the carbon steel, it was also assisted by the interaction of the lone pairs electrons of oxygen atoms and carbon steel surface, as well as the butyl group on the side chains of imidazole rings which increases the hydrophobicity of the compound. Water and other polar compounds contained in the system can lead to the increasing of carbon steel oxidation rate, therefore the water and other polar compounds need to be removed from the system. The more hydrophobic groups in compound **2** are assumed to have responsibility in the formation of more protected sites on carbon steel surface, therefore the metal would be less in contact with the corrosive environments. The increasing of alkyl length on both of compounds leads to the hydrophibicity that would repel water and other polar compounds in the system to be in contact with carbon steel surface, then the corrosion inhibition process would take place effectively and efficiently. The results of the corrosion inhibition activity test showed that compound **2** has more potential as a corrosion inhibitor compares to compound **1**. However, compound **1** has more potential as a corrosion inhibitor than its precursor (2,4,5-triphenylimidazole) [7].

4. CONCLUSIONS

Compound **1** and **2** have been successfully synthesized utilizing MAOS method with chemical yields of 28.12% and 32.18%, respectively. These compounds have potential as corrosion inhibitor.

With the addition of corrosion inhibitors to the system, the activation energy of corrosion process increased and the spontaneity process of corrosion decreased in the inhibited system. The highest activation energy of corrosion process was found in the addition of 20 ppm of compound **2** to the system, which is 49.62 kJ/ mol, which suggests that the corrosion inhibition process runs efficiently at concentration of 20 ppm of compound **2**. The thermodynamic parameters indicate that the addition of corrosion inhibitors inhibit the corrosion rate in the system. Both compounds have potential as corrosion inhibitor, whereas compound **2** is a better corrosion inhibitor than compound **1**.

References

1. O.L.Jr. Riggs, R.M. Hurd, *Corrosion*, 23(8) (1967) 252-258
2. J. Kruger, *Electrochem. Corros.,* The Johns Hopkins University, (2001) 32-34
3. Olivares-Xometl, N.V. Likhanova, M.A. Domı´nguez-Aguilar, J.M. Hallen, L.S. Zamudio and E. Arce, *App. Surf. Sci.*, 252 (2006) 2139–2152
4. A.Chetovani, et.al, *Corr. Sci.*, 45 (2003) 1675-1684.
5. D A Raval, V M Mannari, *Res Ind*, 39 (1994) 94
6. A.M. Al-Mayout, A.K. Al-Amury and Al-Suhybani, *Corr. Sci.*, 57 (2001) 614.
7. D. Wahyuningrum, *Synthesis of Imidazole Derivatives and Determination of Corrosion Inhibition Activity on Carbon Steel Surface*, in *Program Studi Kimia - FMIPA*. 2008, Institut Teknologi Bandung: Bandung.
8. N. D. Abramov and B. V. Trzhtsinskaya, *Chemistry of Heterocyclic Compounds*, *Spinger Link,* 24 (12) (1989) 1309-1321.
9. S. T. Handy and M. Okello, *JOC note*, 70 (5) (2004) 1917-1919.
10. J.Y. Cheng and Y.H. Chu, *Tetrahedron Letters*, 47 (2005) 1575–1579.
11. A.Popova, et al., *Corr. Sci.,* 46 (2004) 1333
12. M.S. Morad and A.M. Kamal El-Dean, *Corr. Sci.,* 48 (2006) 3398
13. N.A. Al-Mobarak, K.F. Khaled, N.H. Mohamed and K.M. Abdel-Azim, *Arabian J. Chem.,* 4 (2) (2010) 185-193.